

Space-time formulation, discretization, and computations for phase-field fracture optimal control problems

D. Khimin¹, M. C. Steinbach¹, and T. Wick^{1,2}

¹Leibniz Universität Hannover, Institut für Angewandte Mathematik, Welfengarten 1, 30167
Hannover, Germany

²Université Paris-Saclay, ENS Paris-Saclay, LMT – Laboratoire de Mécanique et Technologie,
91190 Gif-sur-Yvette, France

Abstract

The purpose of this work is the development of space-time discretization schemes for phase-field optimal control problems. First, a time discretization of the forward problem is derived using a discontinuous Galerkin formulation. Here, a challenge is to include regularization terms and the crack irreversibility constraint. The optimal control setting is formulated by means of the Lagrangian approach from which the primal part, adjoint, tangent and adjoint Hessian are derived. Herein the overall Newton algorithm is based on a reduced approach by eliminating the state constraint. From the low-order discontinuous Galerkin discretization, adjoint time-stepping schemes are finally obtained. Our algorithmic developments are substantiated and illustrated with some numerical experiments.

Keywords:

phase-field fracture propagation; optimal control; reduced optimization approach; finite elements; space-time formulation

AMS:

74R10, 65N30, 49M15, 49K20, 35Q74

1 Introduction

Fracture propagation using variational approaches and phase-field methods is currently an important topic in applied mathematics and engineering. The approach was established in [16, 8] and overview articles and monographs include [9, 10, 41, 40, 15] with numerous further references cited therein. While the major amount of work concentrates on forward modeling of phase-field fracture, more recently some work started on parameter identification employing Bayesian inversion [22, 42, 34, 35], stochastic phase-field modeling [18], and optimal control [32, 33, 31].

The main objective of this work is to design a computational framework for the last topic mentioned, namely phase-field fracture optimal control problems. In prior work [32, 33] the emphasis was on mathematical analysis and a brief illustration in terms of a numerical simulation for a fixed fracture. However, computational details have not yet been discussed therein, but are necessary in order to

apply and investigate the methodology for more practical applications such as propagating fractures. Due to the irreversibility constraint on the fracture growth, optimization problems subject to such an evolution become mathematical programs with complementarity constraints (MPCC) [4, 28, 29] so that standard constraint qualifications like [36, 43] cannot hold. Our computational approach requires stronger regularity and hence we replace the complementarity constraint with a suitable penalty term.

Designing a computational framework for phase-field fracture optimal control is novel and challenging because robust forward and optimization solvers are required. For the forward solver, as intensively discussed in the literature, the linear and nonlinear solutions are demanding because of the non-convexity of the governing energy functional of the forward phase-field fracture model and the relationship of discretization and regularization parameters. For the nonlinear solution various methods were proposed such as alternating minimization (staggered solution) [7, 12], quasi-monolithic solutions [20, 40], and fully monolithic schemes [17, 38, 39, 24, 37]. Nonetheless, monolithic solutions remain difficult and we add an additional viscous regularization term as originally proposed in [23] and used in our governing model from [33]. The optimization problem is formulated in terms of the reduced approach by eliminating the state variable with a control-to-state operator. Therein, Newton-type methods require the evaluation of the *adjoint*, *tangent*, and *adjoint Hessian equations*. The latter requires the evaluation of second-order derivatives; see, e.g., [5] for parabolic optimization problems.

The last paper serves as point of departure for our approach in the current work. Specifically, we employ Galerkin formulations in time and discuss in detail how the crack irreversibility constraint is formulated using a penalization [30, 32] and an additional viscous regularization [33, 23]. Based on these settings, concrete time-stepping schemes are derived. As usual, the primal and tangent problem run forward in time whereas the adjoint and adjoint Hessian equations run backward in time. We then adopt two numerical tests with a given initial notch (fracture) in order to achieve a given fracture path while controlling Neumann boundary traction forces. The main emphasis is to establish robust numerical solver results in terms of the nonlinear forward solver and the nonlinear optimization loop. We notice that propagating fractures within numerical optimization are challenging and were not addressed in the prior work [32, 33]. Some further preliminary results (yet with a stationary, non-propagating fracture) are published in the book chapter [21].

The outline of this paper is as follows: In section 2, the phase-field fracture forward model is introduced. Furthermore, a Galerkin time discretization is provided. Next, in section 3, the optimization problem is stated, including the reduced space approach. In the key section 4 the Lagrangian and three auxiliary equations are carefully derived in great detail. Then, in section 5 two numerical experiments are discussed in order to substantiate our algorithmic developments. Our work is summarized in section 6.

2 Phase-field fracture forward model and space-time discretization

To formulate the forward problem, we first introduce some basic notation and then proceed with a space-time discretization.

2.1 Notation

We consider a bounded domain $\Omega \subset \mathbb{R}^2$. The boundary is partitioned as $\partial\Omega = \Gamma_N \dot{\cup} \Gamma_D$ where both Γ_D and Γ_N have nonzero Hausdorff measure. Next we define two function spaces, $V := H_D^1(\Omega; \mathbb{R}^2) \times H^1(\Omega)$ for the displacement field u and the phase-field φ , and $Q := L^2(\Gamma_N)$ for the control q , where

$$\begin{aligned} H^1(\Omega; \mathbb{R}^2) &:= \{v \in L^2(\Omega; \mathbb{R}^2) : D^\alpha v \in L^2(\Omega; \mathbb{R}^2) \forall \alpha \in \mathbb{N}_0^2, |\alpha| \leq 1\}, \\ H_D^1(\Omega; \mathbb{R}^2) &:= \{v \in H^1(\Omega; \mathbb{R}^2) : v|_{\Gamma_D} = 0\}. \end{aligned}$$

Moreover we consider a bounded time interval $I = [0, T]$ and introduce the spaces

$$X := \{\mathbf{u} = (u, \varphi) : \mathbf{u} \in L^2(I, V), \partial_t \varphi \in L^2(I, H^{-1}(\Omega))\}, \quad W := C(I, Q).$$

On V respectively X we define the scalar products

$$\begin{aligned} (\mathbf{u}, \mathbf{v}) &:= \int_{\Omega} \mathbf{u} \cdot \mathbf{v} \, dx \quad \forall \mathbf{u}, \mathbf{v} \in V, \\ (\mathbf{u}, \mathbf{v})_I &:= \int_I \int_{\Omega} \mathbf{u} \cdot \mathbf{v} \, dx \, dt = \int_I (\mathbf{u}(t), \mathbf{v}(t)) \, dt \quad \forall \mathbf{u}, \mathbf{v} \in X, \end{aligned}$$

with induced norms $\|\cdot\|$ and $\|\cdot\|_I$, and furthermore the restricted inner products

$$\begin{aligned} (\mathbf{u}(t), \mathbf{v}(t))_{\{\partial_t \varphi(t) > 0\}} &:= \begin{cases} (\mathbf{u}(t), \mathbf{v}(t)), & \partial_t \varphi(t) > 0, \\ 0, & \text{else,} \end{cases} \\ (\mathbf{u}, \mathbf{v})_{\{\partial_t \varphi > 0, I\}} &:= \int_I (\mathbf{u}(t), \mathbf{v}(t))_{\{\partial_t \varphi(t) > 0\}} \, dt \quad \forall \mathbf{u}, \mathbf{v} \in X, \end{aligned}$$

with induced semi-norms $\|\cdot\|_{\{\partial_t \varphi > 0\}}$ and $\|\cdot\|_{\{\partial_t \varphi > 0, I\}}$. We also notice that we later work with $(\cdot, \cdot)_{\{\varphi(t_i) > \varphi(t_j)\}}$, defined like $(\cdot, \cdot)_{\{\partial_t \varphi > 0\}}$, and with a semi-linear form $a(\cdot)(\cdot)$ in which the first argument is nonlinear and the second argument is linear.

2.2 Energy functional of quasi-static variational fracture modeling

In the next step we introduce a functional $E_\varepsilon^\gamma : W \times X \rightarrow \mathbb{R}$ from which we derive our forward problem. Here $E_\varepsilon^\gamma(q; u, \varphi)$ is defined as the sum of the regularized total energy of a crack plus a penalty term for the time dependent irreversibility constraint $\partial_t \varphi \leq 0$. The regularized total energy of a crack is given by

$$E_\varepsilon(q; u, \varphi) := \frac{1}{2}(g(\varphi)\mathbb{C}e(u), e(u))_I - (q, u)_{\Gamma_N, I} + G_c \Gamma_\varepsilon(\varphi), \quad (1)$$

where q denotes a force that is applied in orthogonal direction to $\Gamma_N \subset \partial\Omega$, \mathbb{C} is the elasticity tensor and $e(u)$ the symmetric gradient. Then, we have

$$\mathbb{C}e(u) = \sigma(u) = 2\mu e(u) + \lambda \operatorname{tr}(e(u))I,$$

where $\mu, \lambda > 0$ are the Lamé parameters and I is the identity matrix. The so-called degradation function $g(\varphi) := (1 - \kappa)\varphi^2 + \kappa$ helps to extend the displacements to the entire domain Ω . The term $G_c \Gamma_\varepsilon(\varphi) := \frac{1}{2\varepsilon} \|1 - \varphi\|_I + \frac{\varepsilon}{2} \|\nabla \varphi\|_I^2$ is a regularized form of the Hausdorff measure [1]. So far the problem consists in finding a function $\mathbf{u} := (u, \varphi) \in X$ that minimizes the regularized total energy (1) subject

to the irreversibility constraint $\partial_t \varphi \leq 0$. In the sequel, the constraint is being replaced by a penalty term, which is defined as

$$R(\varphi) := \|\partial_t \varphi\|_{\{\partial_t \varphi > 0, I\}}^2.$$

In order to ensure differentiability up to second order, an alternative is to work with a fourth-order penalization [32]. One final modification of E_ε is necessary. We add the convexification term $\frac{\eta}{2}\|\partial_t \varphi\|_I^2$ for some $\eta > 0$. Indeed, in [33], the term $\eta(\varphi^i - \varphi^{i-1}, \psi)$ in time steps $i - 1, i$ was considered for $\eta \geq 0$. This term corresponds to a potential viscous regularization of a rate-independent damage model [23].

Finally the forward problem consists in finding $\mathbf{u} = (u, \varphi) \in X$ that solves the following optimization problem for given initial data $\mathbf{u}_0 = (u_0, \varphi_0) \in V$ and given control $q \in W$:

$$\min_{\mathbf{u}} E_\varepsilon^\gamma(q; u, \varphi) := E_\varepsilon(q; u, \varphi) + \frac{\gamma}{2}R(\varphi) + \frac{\eta}{2}\|\partial_t \varphi\|_I^2, \quad (2)$$

with penalty parameter $\gamma > 0$ and convexification parameter $\eta > 0$.

Remark 2.1 (Initial condition u_0). *Note that we are concerned with quasi-static brittle fracture without explicit time derivative in the displacement equation. Nonetheless, we introduce for formal reasons u_0 . First, we can develop in an analogous fashion time discretization schemes for the overall forward model. Second, it facilitates the extension to problems in which the displacement equation does have a time derivative, such as dynamic fracture [11, 6]. Third, having u_0 allows for a monolithic implementation structure, and the system matrix for the initial condition is regular.*

Remark 2.2 (Convexification). *We notice that strict positivity $\eta > 0$ ensures the required regularity in time, $\partial_t \varphi \in L^2(I, H^{-1}(\Omega))$. Moreover, it improves the numerical solution process of (3). In fact, one can show for the quasi-static case that for sufficiently large values of η the control-to-state mapping associated with (2) is single valued due to strict convexity of the energy corresponding to the equation. However, the convexification term $\frac{\eta}{2}\|\partial_t \varphi\|_I^2$ also penalizes crack growth. To ensure the dominance of the physically motivated term $\frac{\gamma}{2}R(\varphi)$ we have to choose $\gamma \gg \eta$.*

2.3 Weak formulation

Before we continue with the spatial discretization and the concrete time-stepping scheme, we state the weak form of (2). To this end we replace (2) by its first order optimality conditions, see e.g., [32], yielding a coupled nonlinear PDE system: given $\mathbf{u}_0 \in V$ and $q \in W$, find $\mathbf{u} \in X$ such that

$$\begin{aligned} (g(\varphi)\mathbb{C}e(u), e(\Phi_u))_I - (q, \Phi_u)_{\Gamma_N, I} &= 0, \\ G_c \varepsilon (\nabla \varphi, \nabla \Phi_\varphi)_I - \frac{G_c}{\varepsilon} (1 - \varphi, \Phi_\varphi)_I + (1 - \kappa)(\varphi \mathbb{C}e(u) : e(u), \Phi_\varphi)_I & \\ + \gamma (\partial_t \varphi, \Phi_\varphi)_{\{\partial_t \varphi > 0, I\}} + \eta (\partial_t \varphi, \Phi_\varphi)_I &= 0, \end{aligned} \quad (3)$$

for every test function $\Phi = (\Phi_u, \Phi_\varphi) \in X$.

2.4 Galerkin time discretization

Using a time grid $0 = t_0 < \dots < t_M = T$, we first partition the interval I into M left-open subintervals $I_m = (t_{m-1}, t_m]$,

$$I = \{0\} \cup I_1 \cup \dots \cup I_M.$$

By using the discontinuous Galerkin method, here dG(0), we seek for a solution \mathbf{u} in the space X_k^0 of piecewise polynomials of degree 0. The subindex k denotes the time-discretized function space in order to distinguish from the continuous space X . To this end, we have

$$X_k^0 := \{\mathbf{v} \in X : \mathbf{v}|_{I_m} \in \mathbb{P}_0(I_m, V), m = 1, \dots, M \text{ and } \mathbf{v}(0) \in V\}.$$

Remark 2.3. *Since we work with $r = 0$, i.e., constant functions in time, we have*

$$\partial_t \mathbf{v} = \mathbf{v}_m^- - \mathbf{v}_{m-1}^+ = 0 \quad \forall \mathbf{v} \in X_k^0 \text{ and } m = 1, \dots, M.$$

To work with the discontinuities in X_k^0 , we introduce the notation

$$\mathbf{v}_m^+ := \mathbf{v}(t_m+), \quad \mathbf{v}_m^- := \mathbf{v}(t_m-) = \mathbf{v}(t_m), \quad [\mathbf{v}]_m := \mathbf{v}_m^+ - \mathbf{v}_m^-.$$

Now the discretized state equation can be derived from (3) by combining the two equations into a single equation (5). To simplify the notation let us replace the energy-related terms of (3) with a semi-linear form $a: Q \times V \times V \rightarrow \mathbb{R}$,

$$\begin{aligned} a(q, \mathbf{u})(\Phi) &:= g(\varphi) \cdot (\mathbb{C}e(u), e(\Phi_u)) \\ &+ G_c \varepsilon (\nabla \varphi, \nabla \Phi_\varphi) - \frac{G_c}{\varepsilon} (1 - \varphi, \Phi_\varphi) \\ &+ (1 - \kappa) (\varphi \cdot \mathbb{C}e(u) : e(u), \Phi_\varphi) - (q, \Phi_{u,y})_{\Gamma_N}. \end{aligned} \quad (4)$$

Here $\Phi_{u,y}$ denotes the y component of $\Phi_u = (\Phi_{u,x}, \Phi_{u,y})$ in $\Phi = (\Phi_u, \Phi_\varphi) \in V$. Now the fully discretized state equation consists of finding a function $\mathbf{u} \in X_k^0$ for a given control q such that for every $\Phi \in X_k^0$

$$0 = \sum_{m=1}^M [\gamma(\partial_t \varphi, \Phi_\varphi)_{\{\partial_t \varphi > 0, I_m\}} + \eta(\partial_t \varphi, \Phi_\varphi)_{I_m}] \quad (5a)$$

$$+ \sum_{m=0}^{M-1} [\gamma([\varphi]_m, \Phi_{\varphi,m}^+)_{\{\varphi_{m+1}^- > \varphi_m^-\}} + \eta([\varphi]_m, \Phi_{\varphi,m}^+)] \quad (5b)$$

$$+ \sum_{m=1}^M a(q(t_m), \mathbf{u}(t_m))(\Phi(t_m)) \Delta t_m \quad (5c)$$

$$+ (u_0^- - u_0, \Phi_{u,0}^-) + (\varphi_0^- - \varphi_0, \Phi_{\varphi,0}^-). \quad (5d)$$

The time integral in (5c) has been approximated by the right-sided box rule, where $\Delta t_m := t_m - t_{m-1}$. Since the functions in X_k^0 might be discontinuous, we have to add jump terms in the typical dG(0) manner, which are contained in (5b). By expanding these jump terms, (5b) (with index shifted by one) becomes

$$\sum_{m=1}^M [\gamma(\varphi_{m-1}^+ - \varphi_{m-1}^-, \Phi_{\varphi,m-1}^+)_{\{\varphi_m^- > \varphi_{m-1}^-\}} + \eta(\varphi_{m-1}^+ - \varphi_{m-1}^-, \Phi_{\varphi,m-1}^+)]. \quad (6)$$

Now, since we are employing a dG(0) scheme, our test functions satisfy

$$\Phi_{m-1}^+ = \Phi_m^- \quad \forall m = 1, \dots, M.$$

Therefore (5a) vanishes entirely by theorem 2.3, and the two terms containing φ_{m-1}^+ in (6) can be written as $(\varphi_m^-, \Phi_{\varphi,m}^-)_{\{\varphi_m^- > \varphi_{m-1}^-\}}$ and $(\varphi_m^-, \Phi_{\varphi,m}^-)$, respectively. Combining the resulting expression with (5c) and (5d), we finally rewrite (5) as

$$\begin{aligned}
0 = & \sum_{m=1}^M \left(\gamma [(\varphi_m^-, \Phi_{\varphi,m}^-)_{\{\varphi_m^- > \varphi_{m-1}^-\}} - (\varphi_{m-1}^-, \Phi_{\varphi,m}^-)_{\{\varphi_m^- > \varphi_{m-1}^-\}}] \right. \\
& + \eta [(\varphi_m^-, \Phi_{\varphi,m}^-) - (\varphi_{m-1}^-, \Phi_{\varphi,m}^-)] \\
& + a(q(t_m), \mathbf{u}(t_m))(\Phi(t_m))\Delta t_m \Big) \\
& + (u_0^- - u_0, \Phi_{u,0}^-) + (\varphi_0^- - \varphi_0, \Phi_{\varphi,0}^-).
\end{aligned} \tag{7}$$

2.5 Time-stepping scheme

We begin the solution process by solving the last line of (7):

$$\begin{aligned}
(u_0^-, \Phi_{u,0}^-) &= (u_0, \Phi_{u,0}^-), \\
(\varphi_0^-, \Phi_{\varphi,0}^-) &= (\varphi_0, \Phi_{\varphi,0}^-),
\end{aligned} \tag{8}$$

or equivalently $(\mathbf{u}(0), \Phi_0) = (\mathbf{u}_0, \Phi_0)$. Then we proceed and solve for $m = 1, \dots, M$ and every $\Phi \in X_k^0$ the following equation:

$$\begin{aligned}
0 = & \gamma(\varphi(t_m), \Phi_{\varphi}(t_m))_{\{\varphi(t_m) > \varphi(t_{m-1})\}} + \eta(\varphi(t_m), \Phi_{\varphi}(t_m)) \\
& - \gamma(\varphi(t_{m-1}), \Phi_{\varphi}(t_m))_{\{\varphi(t_m) > \varphi(t_{m-1})\}} - \eta(\varphi(t_{m-1}), \Phi_{\varphi}(t_m)) \\
& + a(q(t_m), \mathbf{u}(t_m))(\Phi(t_m))\Delta t_m.
\end{aligned} \tag{9}$$

2.6 Spatial discretization

For the spatial discretization, we employ again a Galerkin finite element scheme by introducing H^1 conforming discrete spaces. We consider two-dimensional shape-regular meshes with quadrilateral elements K forming the mesh $\mathcal{T}_h = \{K\}$; see [13]. The spatial discretization parameter is the diameter h_K of the element K . On the mesh \mathcal{T}_h we construct a finite element space $V_h := V_{uh} \times V_{\varphi h}$ as usual:

$$\begin{aligned}
V_{uh} &:= \{v \in H_D^1(\Omega; \mathbb{R}^2) : v|_K \in Q_s(K) \text{ for } K \in \mathcal{T}_h\}, \\
V_{\varphi h} &:= \{v \in H^1(\Omega) : v|_K \in Q_s(K) \text{ for } K \in \mathcal{T}_h\}.
\end{aligned}$$

Herein $Q_s(K)$ consists of shape functions that are obtained as bilinear transformations of functions defined on the master element $\hat{K} = (0, 1)^2$, where $\hat{Q}_s(\hat{K})$ is the space of tensor product polynomials up to degree s in dimension d defined as

$$\hat{Q}_s(\hat{K}) := \text{span} \left\{ \prod_{i=1}^d \hat{x}_i^{\alpha_i} : \alpha_i \in \{0, 1, \dots, s\} \right\}.$$

Specifically, for $s = 1$ and $d = 2$ we have

$$\hat{Q}_1(\hat{K}) = \text{span}\{1, \hat{x}_1, \hat{x}_2, \hat{x}_1\hat{x}_2\}.$$

We notice for the next two sections that the following derivations are independent of the specific spatial discretization and for this reason the subindex h is omitted.

3 Optimization with phase-field fracture

We formulate the following separable NLP with a tracking type cost functional. For given $(u_0, \varphi_0) \in V$ we seek a solution $(q, \mathbf{u}) \in W \times X_k^0$ of

$$\begin{aligned} \min_{q, \mathbf{u}} \quad \mathcal{J}(q, \mathbf{u}) &:= \frac{1}{2} \sum_{m=1}^M \|\varphi(t_m) - \varphi_d(t_m)\|^2 + \frac{\alpha}{2} \sum_{m=1}^M \|q(t_m) - q_d(t_m)\|_{\Gamma_N}^2 \\ \text{s.t.} \quad (q, \mathbf{u}) &\text{ solves (8) and (9) for } m = 1, \dots, M, \end{aligned} \quad (10)$$

where $\varphi_d \in L^\infty(\Omega)$ is some desired phase-field and q_d is a suitable nominal control that we use for numerical stabilization. The second sum represents a common Tikhonov regularization with the Tikhonov parameter α . The existence of a global solution of (10) in $L^2(I, Q) \times X$ has been shown in [32, Theorem 4.3] for functions that are non-negative and weakly semi-continuous.

3.1 Reduced optimization problem and solution algorithm

We solve (10) by a reduced space approach. To this end, we assume the existence of a solution operator $S: W \rightarrow X$ via equation (3). With this solution operator the cost functional $\mathcal{J}(q, \mathbf{u})$ can be reduced to $j: W \rightarrow \mathbb{R}$, $j(q) := \mathcal{J}(q, S(q))$. As a result we can replace (10) by the unconstrained optimization problem

$$\min_q j(q). \quad (11)$$

The reduced problem is solved by Newton's method applied to $j'(q) = 0$, and hence we need computable representations of the derivatives j' and j'' . The established approach in [5] requires the solution of the following four equations for the Lagrangian $\mathcal{L}(q, \mathbf{u}, \mathbf{z})$; the concrete form is defined in (16).

1. *State equation:* given $q \in W$, find $\mathbf{u} \in X$ such that for all $\Phi \in X$ (3) holds:

$$\mathcal{L}'_{\mathbf{z}}(q, \mathbf{u}, \mathbf{z})(\Phi) = 0. \quad (12)$$

2. *Adjoint equation:* given $q \in W$ and $\mathbf{u} = S(q)$, find $\mathbf{z} \in X$ such that for all $\Phi \in X$

$$\mathcal{L}'_{\mathbf{u}}(q, \mathbf{u}, \mathbf{z})(\Phi) = 0. \quad (13)$$

3. *Tangent equation:* given $q \in W$, $\mathbf{u} = S(q)$ and a direction $\delta q \in W$, find $\delta \mathbf{u} \in X$ such that for all $\Phi \in X$

$$\mathcal{L}''_{q\mathbf{z}}(q, \mathbf{u}, \mathbf{z})(\delta q, \Phi) + \mathcal{L}''_{\mathbf{u}\mathbf{z}}(q, \mathbf{u}, \mathbf{z})(\delta \mathbf{u}, \Phi) = 0. \quad (14)$$

4. *Adjoint Hessian equation:* given $q \in W$, $\mathbf{u} = S(q)$, $\mathbf{z} \in X$ from (13), $\delta \mathbf{u} \in X$ from (14), and a direction $\delta q \in W$, find $\delta \mathbf{z} \in X$ such that for all $\Phi \in X$

$$\mathcal{L}''_{q\mathbf{u}}(q, \mathbf{u}, \mathbf{z})(\delta q, \Phi) + \mathcal{L}''_{\mathbf{u}\mathbf{u}}(q, \mathbf{u}, \mathbf{z})(\delta \mathbf{u}, \Phi) + \mathcal{L}''_{\mathbf{z}\mathbf{u}}(q, \mathbf{u}, \mathbf{z})(\delta \mathbf{z}, \Phi) = 0. \quad (15)$$

Solving these equations in a special order (see for instance [5, 25]) leads to the following representations of the derivatives that we need for Newton's method:

$$\begin{aligned} j'(q)(\delta q) &= \mathcal{L}'_q(q, \mathbf{u}, \mathbf{z})(\delta q) \quad \forall \delta q \in W, \\ j''(q)(\delta q_1, \delta q_2) &= \mathcal{L}''_{qq}(q, \mathbf{u}, \mathbf{z})(\delta q_1, \delta q_2) + \mathcal{L}''_{uq}(q, \mathbf{u}, \mathbf{z})(\delta \mathbf{u}, \delta q_2) \\ &\quad + \mathcal{L}''_{zq}(q, \mathbf{u}, \mathbf{z})(\delta \mathbf{z}, \delta q_2) \quad \forall \delta q_1, \delta q_2 \in W. \end{aligned}$$

4 Lagrangian and auxiliary equations

In the following main section, we specify the previously given abstract formulations in detail. We first derive the Lagrangian and then the three auxiliary equations (13)–(15). Specific emphasis is on the regularization terms for the crack irreversibility and the convexification.

4.1 Lagrangian

We formulate the Lagrangian $\mathcal{L}: W \times X_k^0 \times X_k^0 \rightarrow \mathbb{R}$ within the dG(0) setting as

$$\begin{aligned} \mathcal{L}(q, \mathbf{u}, \mathbf{z}) &:= \mathcal{J}(q, \mathbf{u}) \\ &\quad - \gamma(\partial_t \varphi, z_\varphi)_{\{\partial_t \varphi > 0, I\}} - \eta(\partial_t \varphi, z_\varphi)_I \\ &\quad - \int_I a(q(t), \mathbf{u}(t))(z(t)) \, dt \\ &\quad - \eta_0(u(0) - u_0, z_u(0)) - \eta(\varphi(0) - \varphi_0, z_\varphi(0)). \end{aligned} \tag{16}$$

Note that we have scaled the initial conditions with two different parameters η_0 and η . For the phase-field variable φ we use the convexification parameter of its time derivative to obtain $\eta(\varphi(0) - \varphi_0) = 0$. This is common in the context of a dG(0) setting as it produces desired cancelations with the jump terms resulting from the discontinuities of the test functions. In contrast, the initial condition for u has no physical meaning. Therefore we use a separate parameter $\eta_0 > 0$ to obtain $\eta_0(u(0) - u_0) = 0$. Later we choose $\eta_0 \ll \eta$.

4.2 Adjoint

In the adjoint for $dG(0)$ we seek $\mathbf{z} = (z_u, z_\varphi) \in X_k^0$ such that

$$\mathcal{L}'_{\mathbf{u}}(q, \mathbf{u}, \mathbf{z})(\Phi) = 0 \quad \forall \Phi \in X_k^0.$$

The first interesting part is the calculation of the derivative of \mathcal{L} . We formulate it directly in the weak form

$$\begin{aligned} \mathcal{L}'_{\mathbf{u}}(q, \mathbf{u}, \mathbf{z})(\Phi) &= \mathcal{J}'_{\mathbf{u}}(q, \mathbf{u})(\Phi) \\ &\quad - \gamma(\partial_t \Phi_\varphi, z_\varphi)_{\{\partial_t \varphi > 0, I\}} - \eta(\partial_t \Phi_\varphi, z_\varphi)_I \\ &\quad - \int_I a'_{\mathbf{u}}(q(t), \mathbf{u}(t))(\Phi(t), \mathbf{z}(t)) dt \\ &\quad - \eta_0(\Phi_u(0), z_u(0)) - \eta(\Phi_\varphi(0), z_\varphi(0)). \end{aligned} \tag{17}$$

Herein the partial derivative of a reads

$$\begin{aligned} a'_{\mathbf{u}}(q, \mathbf{u})(\Phi, \mathbf{z}) &= ((1 - \kappa)\varphi^2 + \kappa) \cdot (\mathbb{C}e(\Phi_u), e(z_u)) \\ &\quad + 2\varphi(1 - \kappa)\Phi_\varphi(\mathbb{C}e(u), e(z_u)) \\ &\quad + G_c \varepsilon (\nabla \Phi_\varphi, \nabla z_\varphi) + \frac{G_c}{\varepsilon} (\Phi_\varphi, z_\varphi) \\ &\quad + (1 - \kappa)(\Phi_\varphi \cdot \mathbb{C}e(u) : e(u), z_\varphi) \\ &\quad + 2\varphi(1 - \kappa)(\mathbb{C}e(\Phi_u) : e(u), z_\varphi). \end{aligned} \tag{18}$$

Now the main problem is that the time derivatives are applied to the test function Φ as usual in the adjoint. Therefore we use integration by parts to shift the time derivatives over to \mathbf{z} . Then the second line in (17) becomes

$$\begin{aligned} &\gamma(\Phi_\varphi, \partial_t z_\varphi)_{\{\partial_t \varphi > 0, I\}} + \eta(\Phi_\varphi, \partial_t z_\varphi)_I \\ &+ \gamma(\Phi_\varphi(0), z_\varphi(0))_{\{\partial_t \varphi(0) > 0\}} + \eta(\Phi_\varphi(0), z_\varphi(0)) \\ &- \gamma(\Phi_\varphi(T), z_\varphi(T))_{\{\partial_t \varphi(T) > 0\}} - \eta(\Phi_\varphi(T), z_\varphi(T)). \end{aligned} \tag{19}$$

At this point we have to decide how to approximate the time derivative $\partial_t \varphi(0)$. While $\partial_t \varphi(t_m)$ for $m = 1, \dots, M$ is easily approximated by the backward difference

$$\partial_t \varphi(t_m) \approx \frac{\varphi(t_m) - \varphi(t_{m-1})}{t_m - t_{m-1}},$$

this procedure will not work for the first mesh point $t_0 = 0$. The forward difference

$$\partial_t \varphi(0) \approx \frac{\varphi(t_1) - \varphi(t_0)}{t_1 - t_0}$$

is a good choice because it simplifies the condition $\partial_t \varphi(t_0) > 0$ to $\varphi(t_1) > \varphi(t_0)$ and leads to desired cancelations in (20). Now we will repeat the procedure that we applied to the state equation. We approximate the time derivatives and add the jump terms (with shifted index) as we did in (5),

obtaining expressions similar to (6):

$$\begin{aligned}
\mathcal{L}'_{\mathbf{u}}(q, \mathbf{u}, \mathbf{z})(\Phi) &= \mathcal{J}'_{\mathbf{u}}(q, \mathbf{u})(\Phi) \\
&+ \sum_{m=1}^M [\gamma(\Phi_{\varphi, m}^-, z_{\varphi, m}^- - z_{\varphi, m-1}^+)_{\{\varphi_m^- > \varphi_{m-1}^-\}} \\
&\quad + \eta(\Phi_{\varphi, m}^-, z_{\varphi, m}^- - z_{\varphi, m-1}^+)] \\
&- \gamma(\Phi_{\varphi, M}^-, z_{\varphi, M}^-)_{\{\varphi(t_M) > \varphi(t_{M-1})\}} - \eta(\Phi_{\varphi, M}^-, z_{\varphi, M}^-) \\
&+ \gamma(\Phi_{\varphi, 0}^-, z_{\varphi, 0}^-)_{\{\varphi(t_1) > \varphi(t_0)\}} + \eta(\Phi_{\varphi, 0}^-, z_{\varphi, 0}^-) \\
&+ \sum_{m=1}^M [\gamma(\Phi_{\varphi, m-1}^-, z_{\varphi, m-1}^+ - z_{\varphi, m-1}^-)_{\{\varphi_m^- > \varphi_{m-1}^-\}} \\
&\quad + \eta(\Phi_{\varphi, m-1}^-, z_{\varphi, m-1}^+ - z_{\varphi, m-1}^-)] \\
&- \sum_{m=1}^M a'_{\mathbf{u}}(q(t_m), \mathbf{u}(t_m))(\Phi(t_m), \mathbf{z}(t_m)) \Delta t_m \\
&- \eta_0(\Phi_{u, 0}^-, z_{u, 0}^-) - \eta(\Phi_{\varphi, 0}^-, z_{\varphi, 0}^-).
\end{aligned} \tag{20}$$

Since $z_{\varphi} \in X_k^0$, we have $z_{\varphi, m}^- = z_{\varphi, m-1}^+$ and see that the first sum vanishes entirely. We also see that the terms $\pm \eta(\Phi_{\varphi, 0}^-, z_{\varphi, 0}^-)$ in the fifth and the last line of (20) cancel. Moreover, we assume that $\varphi(t_1) \leq \varphi(t_0)$ in the initial step, and hence the term $-\gamma(\Phi_{\varphi, 0}^-, z_{\varphi, 0}^-)_{\{\varphi(t_1) > \varphi(t_0)\}}$ in the fifth line vanishes as well.

Remark 4.1 (Projection of the initial solution). *The assumption $\varphi(t_1) \leq \varphi(t_0)$ is numerically justified since at t_0 some initial phase-field solution is prescribed. From t_0 to t_1 an L^2 projection of the initial conditions is employed that conserves the crack irreversibility constraint.*

By the above arguments we eliminate the second, third and fifth line of (20) and the second term of the last line, whereas the initial values for z_u are still present:

$$\begin{aligned}
\mathcal{L}'_{\mathbf{u}}(q, \mathbf{u}, \mathbf{z})(\Phi) &= \mathcal{J}'_{\mathbf{u}}(q, \mathbf{u})(\Phi) \\
&- \gamma(\Phi_{\varphi, M}^-, z_{\varphi, M}^-)_{\{\varphi(t_M) > \varphi(t_{M-1})\}} - \eta(\Phi_{\varphi, M}^-, z_{\varphi, M}^-) \\
&+ \sum_{m=1}^M [\gamma(\Phi_{\varphi, m-1}^-, z_{\varphi, m-1}^+ - z_{\varphi, m-1}^-)_{\{\varphi_m^- > \varphi_{m-1}^-\}} \\
&\quad + \eta(\Phi_{\varphi, m-1}^-, z_{\varphi, m-1}^+ - z_{\varphi, m-1}^-)] \\
&- \sum_{m=1}^M a'_{\mathbf{u}}(q(t_m), \mathbf{u}(t_m))(\Phi(t_m), \mathbf{z}(t_m)) \Delta t_m \\
&- \eta_0(\Phi_{u, 0}^-, z_{u, 0}^-).
\end{aligned} \tag{21}$$

4.3 Adjoint time-stepping scheme

From here on we exploit the separable structure of $\mathcal{J}(q, \mathbf{u}) = \sum_m J(q(t_m), \mathbf{u}(t_m))$. We start the solution process by pulling out from (21) every term associated with the last time point t_M :

$$\begin{aligned} & a'_{\mathbf{u}}(q(t_M)\mathbf{u}(t_M))(\Phi(t_M), \mathbf{z}(t_M))\Delta t_M \\ & + \gamma(\Phi_{\varphi, M}^-, z_{\varphi, M}^-)_{\{\varphi_m^- > \varphi_{m-1}^-\}} + \eta(\Phi_{\varphi, M}^-, z_{\varphi, M}^-) \\ & = J'_{\mathbf{u}}(q(t_M), \mathbf{u}(t_M))(\Phi(t_M)) \quad \forall \Phi \in X_k^0. \end{aligned} \quad (22)$$

Now we collect what is left, multiply by -1 and use the X_k^0 property ($z_{\varphi, m-1}^+ = z_{\varphi, m}^-$):

$$\begin{aligned} 0 &= \sum_{m=1}^M \left[\gamma(\Phi_{\varphi, m-1}^-, z_{\varphi, m-1}^- - z_{\varphi, m}^-)_{\{\varphi_m^- > \varphi_{m-1}^-\}} + \eta(\Phi_{\varphi, m-1}^-, z_{\varphi, m-1}^- - z_{\varphi, m}^-) \right] \\ & + \sum_{m=1}^{M-1} a'_{\mathbf{u}}(q(t_m), \mathbf{u}(t_m))(\Phi(t_m), \mathbf{z}(t_m))\Delta t_m \\ & - \sum_{m=1}^{M-1} J'_{\mathbf{u}}(q(t_m), \mathbf{u}(t_m))(\Phi(t_m)) \\ & + \eta_0(\Phi_{u, 0}^-, z_{u, 0}^-) \quad \forall \Phi \in X_k^0. \end{aligned} \quad (23)$$

To formulate the equations that are actually solved in every time step we want to rewrite the entire equation as a single sum. Therefore we shift down the index of the first sum (the jump terms), take out the terms for $m = 0$, and obtain

$$\begin{aligned} 0 &= \sum_{m=1}^{M-1} \left(\left[\gamma(\Phi_{\varphi, m}^-, z_{\varphi, m}^- - z_{\varphi, m+1}^-)_{\{\varphi_{m+1}^- > \varphi_m^-\}} + \eta(\Phi_{\varphi, m}^-, z_{\varphi, m}^- - z_{\varphi, m+1}^-) \right] \right. \\ & \quad \left. + a'_{\mathbf{u}}(q(t_m), \mathbf{u}(t_m))(\Phi(t_m), \mathbf{z}(t_m))\Delta t_m \right. \\ & \quad \left. - J'_{\mathbf{u}}(q(t_m), \mathbf{u}(t_m))(\Phi(t_m)) \right) \\ & + \gamma(\Phi_{\varphi, 0}^-, z_{\varphi, 0}^- - z_{\varphi, 1}^-)_{\{\varphi_1^- > \varphi_0^-\}} + \eta(\Phi_{\varphi, 0}^-, z_{\varphi, 0}^- - z_{\varphi, 1}^-) \\ & + \eta_0(\Phi_{u, 0}^-, z_{u, 0}^-). \end{aligned}$$

Now we solve for $m = M - 1, M - 2, \dots, 1$ the equation

$$\begin{aligned} & a'_{\mathbf{u}}(q(t_m), \mathbf{u}(t_m))(\Phi(t_m), \mathbf{z}(t_m))\Delta t_m \\ & + \gamma(\Phi_{\varphi, m}^-, z_{\varphi, m}^- - z_{\varphi, m+1}^-)_{\{\varphi_{m+1}^- > \varphi_m^-\}} + \eta(\Phi_{\varphi, m}^-, z_{\varphi, m}^- - z_{\varphi, m+1}^-) \\ & = J'_{\mathbf{u}}(q(t_m), \mathbf{u}(t_m))(\Phi(t_m)) \quad \forall \Phi \in X_k^0. \end{aligned}$$

Finally three terms are left for $m = 0$,

$$\gamma(\Phi_{\varphi, 0}^-, z_{\varphi, 0}^- - z_{\varphi, 1}^-)_{\{\varphi_1^- > \varphi_0^-\}} + \eta(\Phi_{\varphi, 0}^-, z_{\varphi, 0}^- - z_{\varphi, 1}^-) + \eta_0(\Phi_{u, 0}^-, z_{u, 0}^-) = 0. \quad (24)$$

For $\eta_0 \ll \eta$ small enough the last term of (24) can be dropped and the following equation can be solved instead:

$$(\Phi_{\varphi, 0}^-, z_{\varphi, 1}^-) = (\Phi_{\varphi, 0}^-, z_{\varphi, 0}^-). \quad (25)$$

Remark 4.2 (Algorithmic realization). *To avoid singular matrices that would lead to a loss of convergence in the linear solvers, we have to add an initial condition for $z_{u,0}^-$: $(\Phi_{u,0}^-, z_{u,1}^-) = (\Phi_{u,0}^-, z_{u,0}^-)$. In total we replace (25) by $(\Phi_0^-, z_1^-) = (\Phi_0^-, z_0^-)$. We also refer the reader to the third reason outlined in theorem 2.1.*

4.4 Tangent equation

The second auxiliary equation is the tangent equation. In this equation we seek $\delta \mathbf{u} = (\delta u, \delta \varphi) \in X_k^0$ such that

$$\mathcal{L}_{qz}''(q, \mathbf{u}, z)(\delta q, \Phi) + \mathcal{L}_{uz}''(q, \mathbf{u}, z)(\delta \mathbf{u}, \Phi) = 0 \quad \forall \Phi \in X_k^0.$$

Here we will apply the same procedure as for the state equation. Recall that $\mathcal{L}(q, \mathbf{u}, z)$ contains the integrand $a(q(t), \mathbf{u}(t))(z(t))$ with $z(t)$ entering linearly. Hence the partial derivative required for $\mathcal{L}_{uz}''(q, \mathbf{u}, z)(\delta \mathbf{u}, \Phi)$ is simply $a'_u(q, \mathbf{u})(\delta \mathbf{u}, \Phi)$, and the partial derivative required for $\mathcal{L}_{qz}''(q, \mathbf{u}, z)(\delta q, \Phi)$ can be derived from (4) as

$$a'_q(q, \mathbf{u})(\delta q, \Phi) = -(\delta q, \Phi_{u;y})_{\Gamma_N}. \quad (26)$$

Furthermore, $\mathcal{J}(q, \mathbf{u})$ does not depend on z , hence \mathcal{J}_{qz}'' and \mathcal{J}_{uz}'' vanish. Using the right-sided box rule again, we thus obtain the discretized tangent equation

$$\begin{aligned} 0 &= \sum_{m=1}^M [\gamma(\delta\varphi_m^- - \delta\varphi_{m-1}^+, \Phi_{\varphi,m}^-)_{\{\varphi_m^- > \varphi_{m-1}^-\}} + \eta(\delta\varphi_m^- - \delta\varphi_{m-1}^+, \Phi_{\varphi,m}^-)] \\ &+ \sum_{m=1}^M a'_u(q(t_m), \mathbf{u}(t_m))(\delta \mathbf{u}(t_m), \Phi(t_m)) \Delta t_m \\ &+ \sum_{m=0}^{M-1} [\gamma(\delta\varphi_m^+ - \delta\varphi_m^-, \Phi_{\varphi,m}^+)_{\{\varphi_{m+1}^- > \varphi_m^-\}} + \eta(\delta\varphi_m^+ - \delta\varphi_m^-, \Phi_{\varphi,m}^+)] \\ &+ \eta_0(\delta u_0^-, \Phi_{u,0}^-) + \eta(\delta\varphi_0^-, \Phi_{\varphi,0}^-) \\ &+ \sum_{m=1}^M a'_q(q(t_m), \mathbf{u}(t_m))(\delta q(t_m), \Phi(t_m)) \Delta t_m \quad \forall \Phi \in X_k^0. \end{aligned} \quad (27)$$

It is clear that the first sum is zero due to the dG(0) property. By shifting the index of the third sum in (27) and applying the dG(0) property to $\Phi_{\varphi,m-1}^+$ we can combine the last three sums and rewrite (27) as

$$\begin{aligned} 0 &= \sum_{m=1}^M \left(a'_u(q(t_m), \mathbf{u}(t_m))(\delta \mathbf{u}(t_m), \Phi(t_m)) \Delta t_m \right. \\ &\quad + \gamma(\delta\varphi_{m-1}^+ - \delta\varphi_{m-1}^-, \Phi_{\varphi,m}^-)_{\{\varphi_m^- > \varphi_{m-1}^-\}} \\ &\quad + \eta(\delta\varphi_{m-1}^+ - \delta\varphi_{m-1}^-, \Phi_{\varphi,m}^-) \\ &\quad \left. + a'_q(q(t_m), \mathbf{u}(t_m))(\delta q(t_m), \Phi(t_m)) \Delta t_m \right) \\ &+ \eta_0(\delta u_0^-, \Phi_{u,0}^-) + \eta(\delta\varphi_0^-, \Phi_{\varphi,0}^-) \quad \forall \Phi \in X_k^0. \end{aligned} \quad (28)$$

4.5 Tangent time-stepping schemes

As in the state equation we first solve the initial conditions,

$$\begin{aligned}(\delta u_0^-, \Phi_{u,0}^-) &= 0, \\ (\delta \varphi_0^-, \Phi_{\varphi,0}^-) &= 0.\end{aligned}$$

Applying the X_k^0 property to $\delta \varphi_{m-1}^+$ we can finally solve for $m = 1, \dots, M$ the following equation

$$\begin{aligned}& \gamma(\delta \varphi_m^-, \Phi_{\varphi,m}^-)_{\{\varphi_m^- > \varphi_{m-1}^-\}} + \eta(\delta \varphi_m^-, \Phi_{\varphi,m}^-) \\ & + a'_u(q(t_m), \mathbf{u}(t_m))(\delta \mathbf{u}(t_m), \Phi(t_m)) \Delta t_m \\ & = (\delta \varphi_{m-1}^-, \Phi_{\varphi,m}^-) + (\delta \varphi_{m-1}^-, \Phi_{\varphi,m}^-)_{\{\varphi_m^- > \varphi_{m-1}^-\}} \\ & - a'_q(q(t_m), \mathbf{u}(t_m))(\delta q(t_m), \Phi(t_m)) \Delta t_m \quad \forall \Phi \in X_k^0.\end{aligned}\tag{29}$$

4.6 Adjoint Hessian equation

The third and last auxiliary equation is the adjoint Hessian equation. In this equation we seek $\delta \mathbf{z} = (\delta z_u, \delta z_\varphi) \in X_k^0$ such that for all $\Phi \in X_k^0$ the following equation holds true:

$$\mathcal{L}''_{qu}(q, \mathbf{u}, \mathbf{z})(\delta q, \Phi) + \mathcal{L}''_{uu}(q, \mathbf{u}, \mathbf{z})(\delta \mathbf{u}, \Phi) + \mathcal{L}''_{zu}(q, \mathbf{u}, \mathbf{z})(\delta \mathbf{z}, \Phi) = 0.\tag{30}$$

First we see that $\mathcal{L}''_{qu}(q, \mathbf{u}, \mathbf{z})(\delta q, \Phi) = 0$ since q and \mathbf{u} are decoupled. The derivative of a in $\mathcal{L}''_{zu}(q, \mathbf{u}, \mathbf{z})(\delta \mathbf{z}, \Phi)$ is given by $a'_u(q, \mathbf{u})(\Phi, \delta \mathbf{z})$ due to the linearity of \mathbf{z} in a . However, a genuine second-order derivative of a arises in $\mathcal{L}''_{uu}(q, \mathbf{u}, \mathbf{z})(\delta \mathbf{u}, \Phi)$:

$$\begin{aligned}a''_{uu}(q, \mathbf{u})(\delta \mathbf{u}, \Phi, \mathbf{z}) &= 2\varphi \cdot (1 - \kappa) \Phi_\varphi \cdot (\mathbb{C}e(\delta u), e(z_u)) \\ & + 2\delta\varphi \cdot (1 - \kappa) (\mathbb{C}e(u), e(z_u)) \cdot \Phi_\varphi \\ & + 2\varphi \cdot (1 - \kappa) (\mathbb{C}e(u), e(z_u)) \delta\varphi \\ & + 2\varphi \cdot (1 - \kappa) (\mathbb{C}e(\Phi_u) : e(\delta u), z_\varphi) \\ & + 2\delta\varphi \cdot (1 - \kappa) (\mathbb{C}e(\Phi_u) : e(u), z_\varphi) \\ & + 2(\mathbb{C}e(\delta u) : e(u), z_\varphi) \cdot \Phi_\varphi.\end{aligned}\tag{31}$$

Now we can rewrite (30) in a dG(0) setting:

$$\begin{aligned}
0 &= \sum_{m=1}^M J''_{\mathbf{u}\mathbf{u}}(q(t_m), \mathbf{u}(t_m))(\delta\mathbf{u}(t_m), \Phi(t_m)) \\
&\quad - \sum_{m=1}^M a''_{\mathbf{u}\mathbf{u}}(q(t_m), \mathbf{u}(t_m))(\delta\mathbf{u}(t_m), \Phi(t_m), \mathbf{z}(t_m))\Delta t_m \\
&\quad + \sum_{m=1}^M [\gamma(\Phi_{\varphi,m}^-, \delta z_{\varphi,m}^- - \delta z_{\varphi,m-1}^+)_{\{\varphi_m^- > \varphi_{m-1}^-\}} + \eta(\Phi_{\varphi,m}^-, z_{\varphi,m}^- - z_{\varphi,m-1}^+)] \\
&\quad - \gamma(\Phi_{\varphi,M}^-, \delta z_{\varphi,M}^-)_{\{\varphi_M^- > \varphi_{M-1}^-\}} - \eta(\Phi_{\varphi,M}^-, \delta z_{\varphi,M}^-) \\
&\quad + \gamma(\Phi_{\varphi,0}^-, \delta z_{\varphi,0}^-)_{\{\varphi_1^- > \varphi_0^-\}} + \eta(\Phi_{\varphi,0}^-, \delta z_{\varphi,0}^-) \\
&\quad - \sum_{m=1}^M a'_{\mathbf{u}}(q(t_m), \mathbf{u}(t_m))(\Phi(t_m), \delta\mathbf{z}(t_m))\Delta t_m \\
&\quad + \sum_{m=0}^{M-1} \gamma(\Phi_{\varphi,m}^-, \delta z_{\varphi,m}^+ - \delta z_{\varphi,m}^-)_{\{\varphi_{m+1}^- > \varphi_m^-\}} + \eta(\Phi_{\varphi,m}^-, \delta z_{\varphi,m}^+ - \delta z_{\varphi,m}^-) \\
&\quad - \eta_0(\Phi_{u,0}^-, \delta z_{u,0}^-) - \eta(\Phi_{\varphi,0}^-, \delta z_{\varphi,0}^-) \quad \forall \Phi \in X_k^0.
\end{aligned} \tag{32}$$

Note that the same scaling of initial data was applied that we already used for the adjoint equation. By the X_k^0 property the third sum vanishes entirely. Due to theorem 4.1 and the cancelation of $\pm\eta(\Phi_{\varphi,0}^-, \delta z_{\varphi,0}^-)$ the fifth line vanishes as well. By shifting the index of the jump terms we can rewrite the equation as:

$$\begin{aligned}
0 &= \sum_{m=1}^M \left(J''_{\mathbf{u}\mathbf{u}}(q(t_m), \mathbf{u}(t_m))(\delta\mathbf{u}(t_m), \Phi(t_m)) \right. \\
&\quad - a''_{\mathbf{u}\mathbf{u}}(q(t_m), \mathbf{u}(t_m))(\delta\mathbf{u}(t_m), \Phi(t_m), \mathbf{z}(t_m))\Delta t_m \\
&\quad - a'_{\mathbf{u}}(q(t_m), \mathbf{u}(t_m))(\Phi(t_m), \delta\mathbf{z}(t_m))\Delta t_m \\
&\quad + \gamma(\Phi_{\varphi,m-1}^-, \delta z_{\varphi,m-1}^+ - \delta z_{\varphi,m-1}^-)_{\{\varphi_m^- > \varphi_{m-1}^-\}} \\
&\quad \left. + \eta(\Phi_{\varphi,m-1}^-, \delta z_{\varphi,m-1}^+ - \delta z_{\varphi,m-1}^-) \right) \\
&\quad - \gamma(\Phi_{\varphi,M}^-, \delta z_{\varphi,M}^-)_{\{\varphi_M^- > \varphi_{M-1}^-\}} - \eta(\Phi_{\varphi,M}^-, \delta z_{\varphi,M}^-) \\
&\quad - \eta_0(\Phi_{u,0}^-, \delta z_{u,0}^-) \quad \forall \Phi \in X_k^0.
\end{aligned} \tag{33}$$

4.7 Adjoint Hessian time-stepping schemes

As in the adjoint time-stepping scheme we first collect all terms that contain the last time point t_M and solve

$$\begin{aligned}
0 &= J''_{\mathbf{u}\mathbf{u}}(q(t_M)\mathbf{u}(t_M))(\delta\mathbf{u}(t_M), \Phi(t_M)) \\
&\quad - a'_{\mathbf{u}}(q(t_M)\mathbf{u}(t_M))(\Phi(t_M), \delta\mathbf{z}(t_M))\Delta t_M \\
&\quad - a''_{\mathbf{u}\mathbf{u}}(q(t_M)\mathbf{u}(t_M))(\delta\mathbf{u}(t_M), \Phi(t_M), \mathbf{z}(t_M))\Delta t_M \\
&\quad - \gamma(\Phi_{\varphi,M}^-, \delta z_{\varphi,M}^-)_{\{\varphi_M^- > \varphi_{M-1}^-\}} - \eta(\Phi_{\varphi,M}^-, \delta z_{\varphi,M}^-) \quad \forall \Phi \in X_k^0.
\end{aligned} \tag{34}$$

Then (33) becomes

$$\begin{aligned}
0 = & \sum_{m=1}^{M-1} \left(J''_{\mathbf{u}\mathbf{u}}(q(t_m), \mathbf{u}(t_m))(\delta\mathbf{u}(t_m), \Phi(t_m)) \right. \\
& - a''_{\mathbf{u}\mathbf{u}}(q(t_m), \mathbf{u}(t_m))(\delta\mathbf{u}(t_m), \Phi(t_m), \mathbf{z}(t_m))\Delta t_m \\
& \left. - a'_{\mathbf{u}}(q(t_m), \mathbf{u}(t_m))(\Phi(t_m), \delta\mathbf{z}(t_m))\Delta t_m \right) \\
& + \sum_{m=1}^M \left(\gamma(\Phi_{\varphi, m-1}^-, \delta z_{\varphi, m-1}^+ - \delta z_{\varphi, m-1}^-)_{\{\varphi_m^- > \varphi_{m-1}^-\}} \right. \\
& \quad \left. + \eta(\Phi_{\varphi, m-1}^-, \delta z_{\varphi, m-1}^+ - \delta z_{\varphi, m-1}^-) \right) \\
& - \eta_0(\Phi_{u, 0}^-, \delta z_{u, 0}^-) \quad \forall \Phi \in X_k^0.
\end{aligned} \tag{35}$$

In the final reformulation we shift the index of the second sum (jump-terms) and take out the terms corresponding to $m = 0$

$$\begin{aligned}
0 = & \sum_{m=1}^{M-1} \left(J''_{\mathbf{u}\mathbf{u}}(q(t_m), \mathbf{u}(t_m))(\delta\mathbf{u}(t_m), \Phi(t_m)) \right. \\
& - a''_{\mathbf{u}\mathbf{u}}(q(t_m), \mathbf{u}(t_m))(\delta\mathbf{u}(t_m), \Phi(t_m), \mathbf{z}(t_m))\Delta t_m \\
& - a'_{\mathbf{u}}(q(t_m), \mathbf{u}(t_m))(\Phi(t_m), \delta\mathbf{z}(t_m))\Delta t_m \\
& + \gamma(\Phi_{\varphi, m}^-, \delta z_{\varphi, m}^+ - \delta z_{\varphi, m}^-)_{\{\varphi_{m+1}^- > \varphi_m^-\}} \\
& \left. + \eta(\Phi_{\varphi, m}^-, \delta z_{\varphi, m}^+ - \delta z_{\varphi, m}^-) \right) \\
& + \gamma(\Phi_{\varphi, 0}^-, \delta z_{\varphi, 0}^+ - \delta z_{\varphi, 0}^-)_{\{\varphi_1^- > \varphi_0^-\}} + \eta(\Phi_{\varphi, 0}^-, \delta z_{\varphi, 0}^+ - \delta z_{\varphi, 0}^-) \\
& - \eta_0(\Phi_{u, 0}^-, \delta z_{u, 0}^-) \quad \forall \Phi \in X_k^0.
\end{aligned} \tag{36}$$

As already pointed out in the time-stepping scheme for the adjoint equation, all dual equations have to be solved backwards in time. Therefore, we solve the following equation for $m = M-1, M-2, \dots, 1$

$$\begin{aligned}
0 = & J''_{\mathbf{u}\mathbf{u}}(q(t_m), \mathbf{u}(t_m))(\delta\mathbf{u}(t_m), \Phi(t_m)) \\
& - a''_{\mathbf{u}\mathbf{u}}(q(t_m), \mathbf{u}(t_m))(\delta\mathbf{u}(t_m), \Phi(t_m), \mathbf{z}(t_m))\Delta t_m \\
& - a'_{\mathbf{u}}(q(t_m), \mathbf{u}(t_m))(\Phi(t_m), \delta\mathbf{z}(t_m))\Delta t_m \\
& + \gamma(\Phi_{\varphi, m}^-, \delta z_{\varphi, m}^+ - \delta z_{\varphi, m}^-)_{\{\varphi_{m+1}^- > \varphi_m^-\}} \\
& + \eta(\Phi_{\varphi, m}^-, \delta z_{\varphi, m}^+ - \delta z_{\varphi, m}^-) \quad \forall \Phi \in X_k^0.
\end{aligned}$$

As a result, the only remaining terms in (36) are

$$\gamma(\Phi_{\varphi, 0}^-, \delta z_{\varphi, 0}^+ - \delta z_{\varphi, 0}^-)_{\{\varphi_1^- > \varphi_0^-\}} + \eta(\Phi_{\varphi, 0}^-, \delta z_{\varphi, 0}^+ - \delta z_{\varphi, 0}^-) - \eta_0(\Phi_{u, 0}^-, \delta z_{u, 0}^-). \tag{37}$$

Finally we can apply the assumption $\eta_0 \ll \eta$ once more and drop the last term in (37). Consequently the following equations have to be solved for all $\Phi \in X_k^0$:

$$\begin{aligned}
(\Phi_{\varphi, 0}^-, \delta z_{\varphi, 0}^-) &= (\Phi_{\varphi, 0}^-, \delta z_{\varphi, 1}^-), \\
(\Phi_{u, 0}^-, \delta z_{u, 0}^-) &= (\Phi_{u, 0}^-, \delta z_{u, 1}^-).
\end{aligned}$$

Note that theorem 4.2 was applied to (37) as well.

5 Numerical tests

In the following section we present two numerical examples for the optimal control problem. In these examples we use the tracking type functional of (10) to find an optimal control that approximately produces a desired phase-field. All numerical computations are performed with the open source software libraries `deal.II` [2, 3] and `DOPELIB` [14, 19].

For both examples we consider the square domain $\Omega = (0, 1)^2$ with a horizontal notch, see section 5.



Figure 1: Domain $\Omega = (0, 1)^2$ with partitioned boundary $\partial\Omega$, initial notch, and desired crack φ_d .

Table 1: Regularization and penalty parameters (left) and model parameters (right).

Par.	Definition	Value	Par.	Definition	Value
ε_1	Regul. (crack) $\approx 4h_1$	0.0884	G_c	Fracture toughness	1.0
ε_2	Regul. (crack) $\approx 4h_2$	0.0442	ν_s	Poisson's ratio	0.2
κ	Regul. (crack)	1.00e-10	E	Young's modulus	1.0e6
η	Regul. (viscosity)	1.00e3	q_0	Initial control	1.0
γ	Penalty	1.00e5	q_{d1}	Nominal control	1.0e3
α_1	Tikhonov	4.75e-10	q_{d2}	Nominal control	3.0e3
α_2	Tikhonov	1.00e-10			

In Example 1 the notch is in the middle of the right side, defined as $(0.5, 1) \times \{0.5\}$, in Example 2 it is in the middle of Ω , defined as $(0.25, 0.75) \times \{0.5\}$. The boundary $\partial\Omega$ is partitioned as $\partial\Omega = \Gamma_N \cup \Gamma_D \cup \Gamma_{\text{free}}$, where $\Gamma_N := [0, 1] \times \{1\}$, $\Gamma_D := [0, 1] \times \{0\}$, and $\Gamma_{\text{free}} := \{0, 1\} \times (0, 1)$. On Γ_N we apply the force q in orthogonal direction to the domain and on Γ_D we enforce Dirichlet boundary conditions for the displacement $u = 0$. We choose the time interval $[0, 1]$ with 41 equidistant time points t_m , i.e. $T = 1$ and $M = 40$. The control space Q_h (the spatial discretization of Q) is one-dimensional in the sense that the force is only applied in y -direction and is constant in time, $q(t_m) = q$. The spatial mesh consists of 64×64 square elements in Example 1 and 128×128 square elements in Example 2, hence the element diameter is $h_1 = \sqrt{2}/64$ and $h_2 = \sqrt{2}/128$, respectively. The initial data is given

by $\mathbf{u}_0 = (u_0, \varphi_0)$ where φ_0 describes the horizontal notch,

$$\varphi_0(x, y) := \begin{cases} 0, & x \in (0.50, 1.00) \text{ and } y = 0.5 \text{ (Example 1)}, \\ 0, & x \in (0.25, 0.75) \text{ and } y = 0.5 \text{ (Example 2)}, \\ 1, & \text{else.} \end{cases} \quad (38)$$

The desired phase-field φ_d continues the initial notch to the left,

$$\varphi_d(x, y) := \begin{cases} 0, & x \in (0.25, 0.5) \text{ and } y \in (0.5 - h_1, 0.5 + h_1) \text{ (Example 1)}, \\ 0, & x \in (0, 0.25) \text{ and } y \in (0.5 - 2h_2, 0.5 + 2h_2) \text{ (Example 2)}, \\ 1, & \text{else.} \end{cases} \quad (39)$$

The parameters used in our numerical tests are given in section 5. Note that ε , α , and the constant nominal control q_d differ for the two examples while the crack widths that we prescribe via φ_d agree: $2h_2 = h_1$ in (39).

5.1 Example 1: horizontal fracture in right half domain

The first example is motivated by a standard problem: the single edge notched tension test [27, 26]; see again section 5. Our results are presented in section 5.1. The first column (Iter) gives the iteration index of Newton's method in solving the reduced problem (11). The second column (CG) gives the number of CG iterations required for computing the Newton increment. The remaining values are the relative and absolute Newton residuals, the cost functional \mathcal{J} and its tracking part $\frac{1}{2} \sum_{m=1}^M \|\varphi(t_m) - \varphi_d(t_m)\|^2$, the maximal force $|q_{\max}|$ applied on Γ_N , and finally the Tikhonov regularization term, $\frac{\alpha}{2} \sum_{m=1}^M \|q(t_m) - q_d(t_m)\|_{\Gamma_N}^2$. All values are rounded to three or five significant digits.

The Newton iteration terminates when the relative residual or the absolute residual falls below the tolerance $2e-12$. Optimal phase-fields, displacements, adjoints, and forces are presented in section 5.1. The optimal force on $\Gamma_N = [0, 1] \times \{1\}$ grows almost linearly from 745.3 at $(0, 1)$ to 2473.4 at $(1, 1)$.

As a side-note, we observed within our computations that it is quite challenging to entirely reach the desired crack φ_d . This is clear since we have the usual competition between the physics given by the tracking functional and the numerical regularization given by the Tikhonov term. Of course, with α chosen sufficiently well and a well-guessed q_d we could place a higher weight on the regularization to track the desired fracture path better. On the other hand, to control a propagating fracture at all has not yet been achieved in the published literature to the best of our knowledge.

5.2 Example 2: horizontal fracture in the middle

The second example is motivated by the question whether it is possible to produce a one sided crack growth. The desired phase-field φ_d continues the initial notch only to the left boundary, see again section 5, but the right fracture tip should not move. For that reason, this numerical experiment differs quite significantly from the first configuration in the behavior of the numerical solution as well as the final fracture path outcomes.

Table 2: Results of Example 1: numerical solver performance, convergence of functionals, and evolution of control forces.

Iter	CG	Relative residual	Absolute residual	Cost	Tracking	Tikhonov	Force
0	—	1.0	4.62e-7	5.1630e-3	4.9289e-3	2.3406e-4	1.0
1	3	0.464	2.14e-7	4.7699e-3	4.7699e-3	3.2317e-9	1001.2
2	3	0.207	9.56e-8	4.5782e-3	4.5276e-3	5.0571e-5	1899.7
3	3	0.106	4.88e-8	4.4968e-3	4.3911e-3	1.0570e-4	2308.1
4	3	2.73e-3	1.26e-9	4.4600e-3	4.3186e-3	1.4137e-4	2498.9
5	10	7.18e-4	3.32e-10	4.4606e-3	4.3203e-3	1.4032e-4	2469.5
6	5	2.93e-4	1.35e-10	4.4592e-3	4.3174e-3	1.4183e-4	2471.1
7	5	1.03e-4	4.73e-11	4.4585e-3	4.3159e-3	1.4258e-4	2473.1
8	3	4.44e-5	2.05e-11	4.4584e-3	4.3156e-3	1.4273e-4	2473.0
9	3	1.54e-5	7.09e-12	4.4583e-3	4.3154e-3	1.4286e-4	2473.4
10	2	3.78e-6	1.75e-12	4.4582e-3	4.3153e-3	1.4289e-4	2473.4

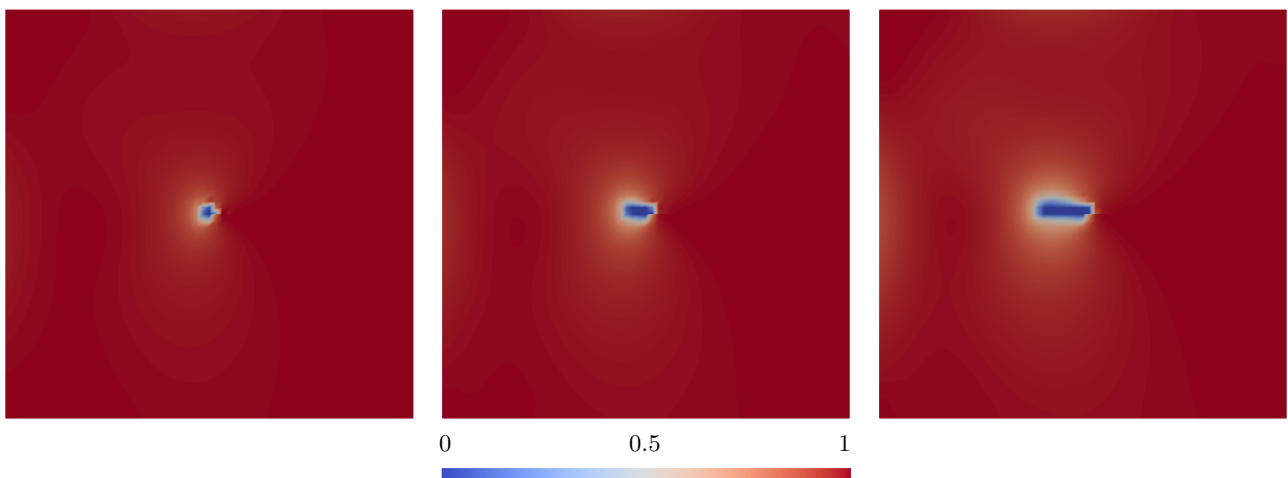


Figure 2: Example 1: optimal phase-field φ at times 20, 30, and 40.

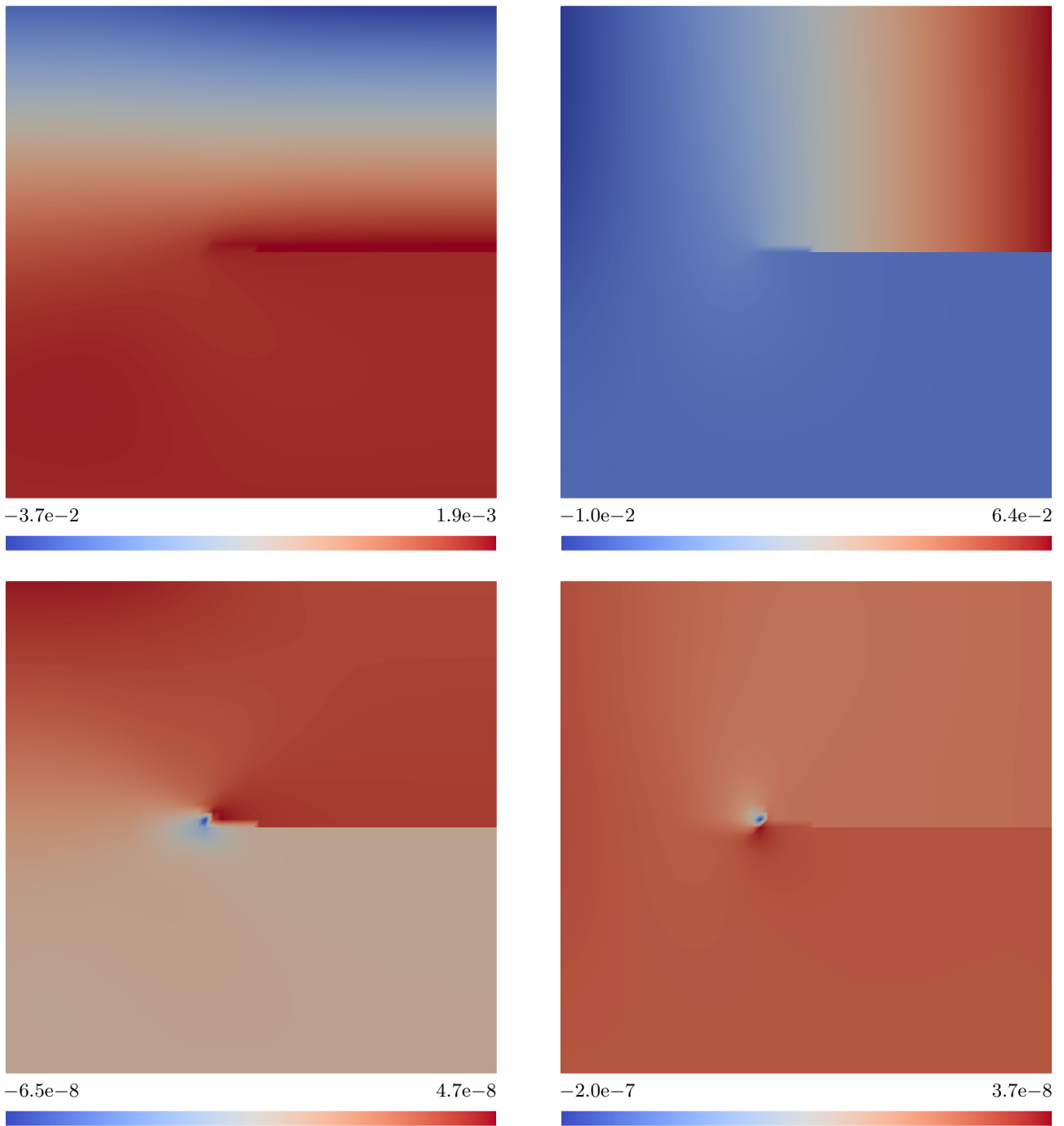


Figure 3: Example 1: optimal displacement field u (top: x left, y right) and adjoint field z_u (bottom: x left, y right) at time 40.

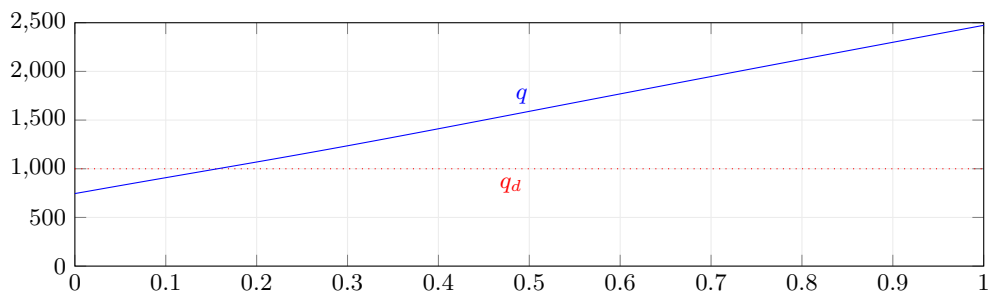


Figure 4: Example 1: optimal control force (solid) and nominal control force (dotted) on upper boundary $\Gamma_N = [0, 1] \times \{1\}$.

Table 3: Results of Example 2: numerical solver performance, convergence of functionals, and evolution of control forces.

Iter	CG	Relative residual	Absolute residual	Cost	Tracking	Tikhonov	Force
0	—	1.0	2.92e-7	1.1481e-2	1.1037e-2	4.4409e-4	1.0
1	3	0.475	1.39e-7	1.0703e-2	1.0703e-2	2.0512e-9	3001.0
2	3	0.280	8.17e-8	1.0308e-2	1.0208e-2	1.0027e-4	5542.4
3	3	0.011	3.21e-9	1.0068e-2	9.8146e-3	2.5294e-4	7051.8
4	14	2.02e-3	5.89e-10	9.9970e-3	9.6262e-3	3.4301e-4	7698.9
5	11	3.59e-4	1.05e-10	9.9953e-3	9.5933e-3	3.5995e-4	7767.2
6	9	2.14e-4	6.26e-11	9.9951e-3	9.5880e-3	3.6268e-4	7788.6
7	6	1.60e-4	4.66e-11	9.9949e-3	9.5855e-3	3.6402e-4	7791.8
8	8	1.07e-4	3.12e-11	9.9948e-3	9.5827e-3	3.6542e-4	7802.2
9	5	6.93e-5	2.02e-11	9.9947e-3	9.5811e-3	3.6625e-4	7805.3
10	6	4.32e-5	1.26e-11	9.9947e-3	9.5799e-3	3.6688e-4	7809.6
11	4	2.99e-5	8.73e-12	9.9946e-3	9.5792e-3	3.6723e-4	7810.9

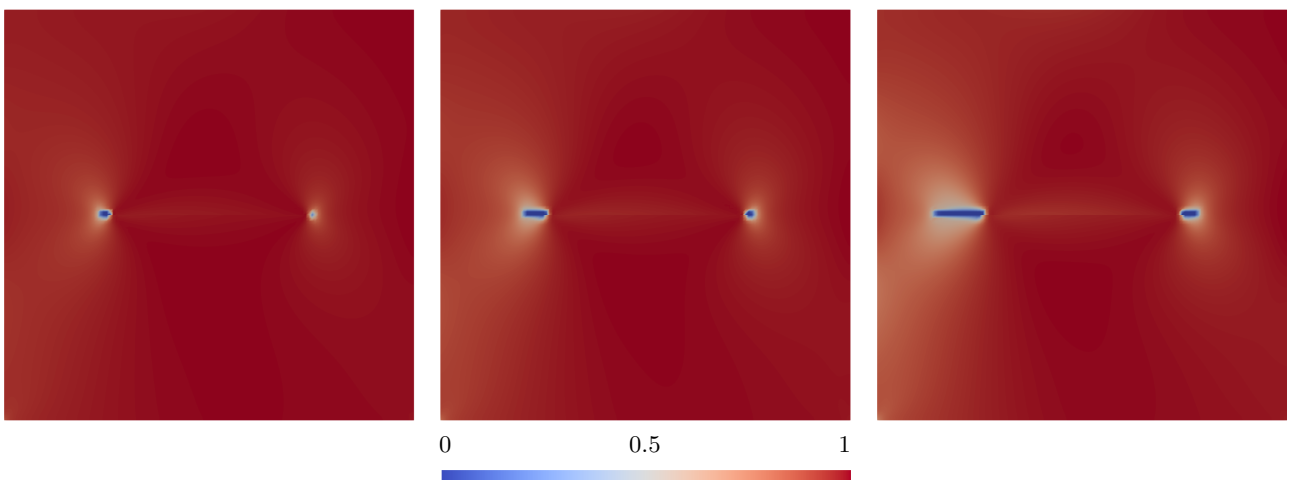


Figure 5: Example 2: optimal phase-field φ at times 20, 30, and 40.

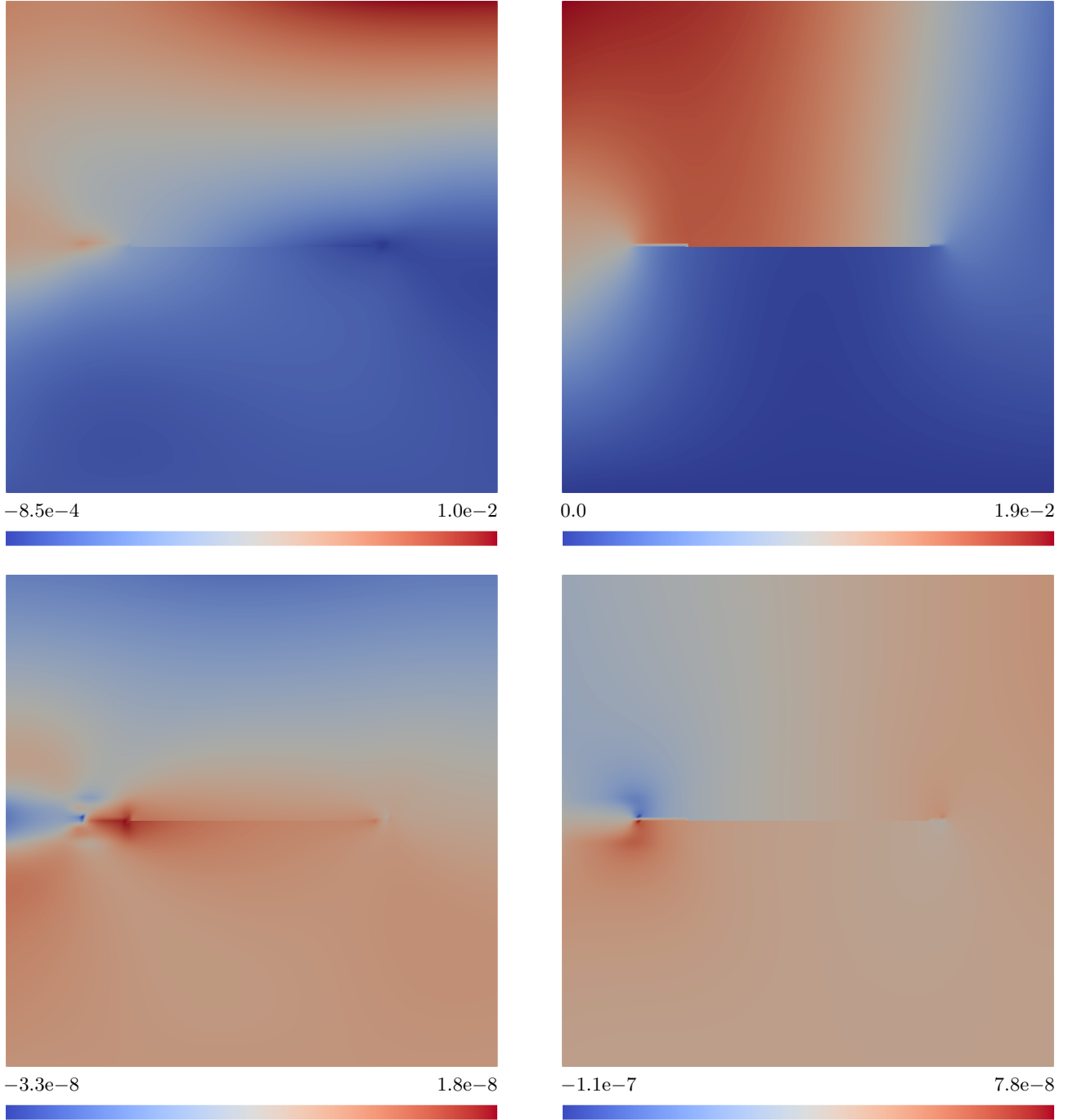


Figure 6: Example 2: optimal displacement field u (top: x left, y right) and adjoint field z_u (bottom: x left, y right) at time 40.

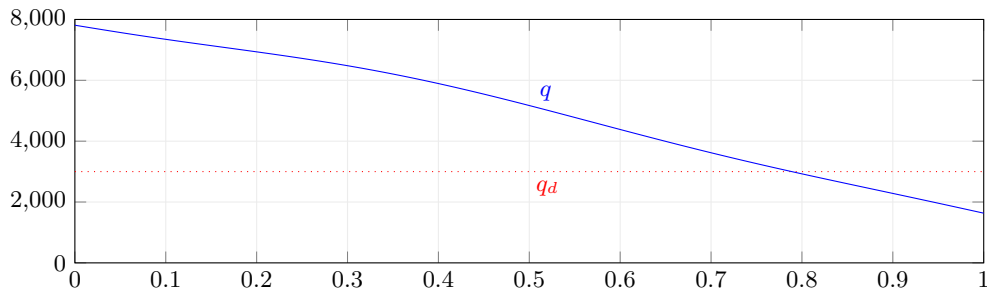


Figure 7: Example 2: optimal control force (solid) and nominal control force (dotted) on upper boundary $\Gamma_N = [0, 1] \times \{1\}$.

Our results are presented in sections 5.1 to 5.2. Here the tolerance for Newton’s method is $1e-11$. The qualitative performance of each numerical solver is similar to Example 1. Concerning the optimal fracture path (phase-field in section 5.2) we obtain the desired solution, namely crack growth starting from the left fracture tip. In the rightmost subfigure of section 5.2, however, we also observe a slight movement of the right fracture tip. This is reasonable because the optimal traction still has a physical impact on the overall fracture and the cost functional is only enforced up to numerical regularization and discretization approximation qualities. The optimal force now decreases from 7810.9 at $(0, 1)$ to 1633.6 at $(1, 1)$.

6 Conclusions

In this paper we derived a space-time Galerkin formulation for a regularized phase-field fracture optimal control setting. By introducing jump terms in time and with the help of a discontinuous Galerkin discretization in time, specific time-stepping schemes could be obtained. A careful investigation of correct weighting of two regularization terms and the initial conditions was necessary for the forward phase-field fracture problem. The solution process of the optimization problem was based on the reduced approach in which the state variables are obtained from a solution operator acting on the controls. The numerical solution algorithm is based on Newton’s method in which three auxiliary problems are required. The main part of the paper was concerned with the detailed derivation of these terms, which are to the best of our knowledge novel in the published literature. We then discussed two numerical tests in order to show the performance of our framework. Therein, we studied the convergence of the residuals (relative and absolute) of the reduced problem, the number of Newton steps and CG iterations as well as the behavior of the cost functional. These findings indicate the robustness and suitability of our numerical solvers to address optimal control phase-field with propagating fractures. Graphical results of the phase-field solution (showing the fracture path) and the optimal displacement field illustrate our findings.

7 Acknowledgements

The first and third author are partially funded by the Deutsche Forschungsgemeinschaft (DFG, German Research Foundation) Priority Program 1962 (DFG SPP 1962) within the subproject *Optimizing Fracture Propagation using a Phase-Field Approach* with the project number 314067056. The second author is funded by the DFG – SFB1463 – 434502799.

References

- [1] L. Ambrosio and V. Tortorelli. On the approximation of free discontinuity problems. *Boll. Un. Mat. Ital. B*, 6:105–123, 1992.
- [2] D. ARNDT, W. BANGERTH, T. C. CLEVINGER, D. DAVYDOV, M. FEHLING, D. GARCIA-SANCHEZ, G. HARPER, T. HEISTER, L. HELTAI, M. KRONBICHLER, R. M. KYNCH, M. MAIER, J.-P. PELTERET, B. TURCK SIN, AND D. WELLS, *The deal.II library, version 9.1*, Journal of Numerical Mathematics, (2019), <https://doi.org/10.1515/jnma-2019-0064>, <https://dealii.org/deal91-preprint.pdf>.
- [3] D. ARNDT, W. BANGERTH, D. DAVYDOV, T. HEISTER, L. HELTAI, M. KRONBICHLER, M. MAIER, J.-P. PELTERET, B. TURCK SIN, AND D. WELLS, *The deal.II finite element library: Design, features, and insights*, Computers & Mathematics with Applications, (2020), <https://doi.org/10.1016/j.camwa.2020.02.022>, <http://www.sciencedirect.com/science/article/pii/S0898122120300894>.
- [4] V. P. Barbu. *Optimal Control of Variational Inequalities*, volume 100. Pitman Advanced Pub. Program, 1984.
- [5] R. Becker, D. Meidner, and B. Vexler. Efficient numerical solution of parabolic optimization problems by finite element methods. *Optim. Methods Softw.*, 22(5):813–833, 2007.
- [6] M. J. Borden, C. V. Verhoosel, M. A. Scott, T. J. R. Hughes, and C. M. Landis. A phase-field description of dynamic brittle fracture. *Comput. Meth. Appl. Mech. Engrg.*, 217:77–95, 2012.
- [7] B. Bourdin. Numerical implementation of the variational formulation for quasi-static brittle fracture. *Interfaces and free boundaries*, 9:411–430, 2007.
- [8] B. Bourdin, G. Francfort, and J.-J. Marigo. Numerical experiments in revisited brittle fracture. *J. Mech. Phys. Solids*, 48(4):797–826, 2000.
- [9] B. Bourdin, G. Francfort, and J.-J. Marigo. The variational approach to fracture. *J. Elasticity*, 91(1–3):1–148, 2008.
- [10] B. Bourdin and G. A. Francfort. Past and present of variational fracture. *SIAM News*, 52(9), 2019.

- [11] B. Bourdin, C. Larsen, and C. Richardson. A time-discrete model for dynamic fracture based on crack regularization. *Int. J. Frac.*, 168(2):133–143, 2011.
- [12] S. Burke, C. Ortner, and E. Süli. An adaptive finite element approximation of a variational model of brittle fracture. *SIAM J. Numer. Anal.*, 48(3):980–1012, 2010.
- [13] P. G. Ciarlet. *The Finite Element Method for Elliptic Problems*. North-Holland, Amsterdam [u.a.], 2. pr. edition, 1987.
- [14] *The Differential Equation and Optimization Environment: DOPELIB*, <http://www.dopelib.net>. <http://www.dopelib.net>.
- [15] G. Francfort. Variational fracture: Twenty years after. *International Journal of Fracture*, pages 1–11, 2021.
- [16] G. Francfort and J.-J. Marigo. Revisiting brittle fracture as an energy minimization problem. *J. Mech. Phys. Solids*, 46(8):1319–1342, 1998.
- [17] T. Gerasimov and L. D. Lorenzis. A line search assisted monolithic approach for phase-field computing of brittle fracture. *Computer Methods in Applied Mechanics and Engineering*, 312:276–303, 2016.
- [18] T. Gerasimov, U. Römer, J. Vondřejc, H. G. Matthies, and L. De Lorenzis. Stochastic phase-field modeling of brittle fracture: Computing multiple crack patterns and their probabilities. *Computer Methods in Applied Mechanics and Engineering*, 372:113353, 2020.
- [19] C. GOLL, T. WICK, AND W. WOLLNER, *DOPElib: Differential equations and optimization environment; A goal oriented software library for solving pdes and optimization problems with pdes*, *Archive of Numerical Software*, 5 (2017), pp. 1–14, <https://doi.org/10.11588/ans.2017.2.11815>.
- [20] T. Heister, M. F. Wheeler, and T. Wick. A primal-dual active set method and predictor-corrector mesh adaptivity for computing fracture propagation using a phase-field approach. *Comp. Meth. Appl. Mech. Engrg.*, 290:466–495, 2015.
- [21] D. Khimin, M. C. Steinbach, and T. Wick. Optimal control for phase-field fracture: Algorithmic concepts and computations. In F. Aldakheel, B. Hudobivnik, M. Soleimani, H. Wessels, C. Weißenfels, and M. Marino, editors, *Current Trends and Open Problems in Computational Mechanics*. Springer, 2021. In press.
- [22] A. Khodadadian, N. Nohi, M. Parvizi, M. Abbaszadeh, T. Wick, and C. Heitzinger. A Bayesian estimation method for variational phase-field fracture problems. *Computational Mechanics*, 66:827–849, 2020.
- [23] D. Knees, R. Rossi, and C. Zanini. A vanishing viscosity approach to a rate-independent damage model. *Mathematical Models and Methods in Applied Sciences*, 23(04):565–616, 2013.

- [24] A. Kopanicakova and R. Krause. A recursive multilevel trust region method with application to fully monolithic phase-field models of brittle fracture. *Computer Methods in Applied Mechanics and Engineering*, 360:112720, 2020.
- [25] D. Meidner. *Adaptive Space-Time Finite Element Methods for Optimization Problems Governed by Nonlinear Parabolic Systems*. PhD thesis, University of Heidelberg, 2008.
- [26] C. MIEHE, M. HOFACKER, AND F. WELSCHINGER, *A phase field model for rate-independent crack propagation: Robust algorithmic implementation based on operator splits*, *Comput. Meth. Appl. Mech. Engrg.*, 199 (2010), pp. 2765–2778.
- [27] C. MIEHE, F. WELSCHINGER, AND M. HOFACKER, *Thermodynamically consistent phase-field models of fracture: variational principles and multi-field fe implementations*, *Int. J. Numer. Methods Engrg.*, 83 (2010), pp. 1273–1311.
- [28] F. Mignot. Contrôle dans les inéquations variationnelles elliptiques. *Journal of Functional Analysis*, 22(2):130–185, 1976.
- [29] F. Mignot and J. P. Puel. Optimal control in some variational inequalities. 22(3):466–476, May 1984.
- [30] A. Mikelić, M. Wheeler, and T. Wick. A phase-field approach to the fluid filled fracture surrounded by a poroelastic medium. ICES Report 13-15, Jun 2013.
- [31] M. Mohammadi and W. Wollner. Phase field modelling of fracture. *Optimization and Engineering*, 2020.
- [32] I. Neitzel, T. Wick, and W. Wollner. An optimal control problem governed by a regularized phase-field fracture propagation model. *SIAM Journal on Control and Optimization*, 55(4):2271–2288, 2017.
- [33] I. Neitzel, T. Wick, and W. Wollner. An optimal control problem governed by a regularized phase-field fracture propagation model. Part II: The regularization limit. *SIAM Journal on Control and Optimization*, 57(3):1672–1690, 2019.
- [34] N. Noh, A. Khodadadian, J. Ulloa, F. Aldakheel, T. Wick, S. Francois, and P. Wriggers. Bayesian inversion for unified ductile phase-field fracture. *Computational Mechanics*, 2021.
- [35] N. Noh, A. Khodadadian, and T. Wick. Bayesian inversion for anisotropic hydraulic phase-field fracture. *Computer Methods in Applied Mechanics and Engineering*, 386:114–118, 2021.
- [36] S. M. Robinson. Stability theory for systems of inequalities, part ii: Differentiable nonlinear systems. *SIAM Journal on Numerical Analysis*, 13(4):497–513, 1976.
- [37] J. Wambacq, J. Ulloa, G. Lombaert, and S. François. Interior-point methods for the phase-field approach to brittle and ductile fracture, 2020.

- [38] T. Wick. An error-oriented Newton/inexact augmented Lagrangian approach for fully monolithic phase-field fracture propagation. *SIAM Journal on Scientific Computing*, 39(4):B589–B617, 2017.
- [39] T. Wick. Modified Newton methods for solving fully monolithic phase-field quasi-static brittle fracture propagation. *Computer Methods in Applied Mechanics and Engineering*, 325:577–611, 2017.
- [40] T. Wick. *Multiphysics Phase-Field Fracture: Modeling, Adaptive Discretizations, and Solvers*. De Gruyter, Berlin, Boston, 2020.
- [41] J.-Y. Wu, V. P. Nguyen, C. Thanh Nguyen, D. Sutula, S. Bordas, and S. Sinaie. Phase field modelling of fracture. *Advances in Applied Mechanics*, 53:1–183, 09 2020.
- [42] T. Wu, B. Rosic, L. de Lorenzis, and H. Matthies. Parameter identification for phase-field modeling of fracture: a Bayesian approach with sampling-free update. *Computational Mechanics*, 67:435–453, 2021.
- [43] J. Zowe and S. Kurcyusz. Regularity and stability for the mathematical programming problem in banach spaces. *Applied Mathematics and Optimization*, 5(1):49–62, Mar. 1979.